

# Effects of pressure on the band structure of highly mismatched $\text{Zn}_{1-y}\text{Mn}_y\text{O}_x\text{Te}_{1-x}$ alloys

W. Shan,<sup>a)</sup> K. M. Yu, W. Walukiewicz, J. W. Beeman, J. Wu, J. W. Ager III, M. A. Scarpulla,<sup>b)</sup> O. D. Dubon,<sup>b)</sup> and E. E. Haller<sup>b)</sup>

Materials Sciences Division, Lawrence Berkeley National Laboratory, Berkeley, California 94720

(Received 4 September 2003; accepted 15 December 2003)

We report photomodulation spectroscopy measurements of the pressure dependence of the optical transition in  $\text{Zn}_{1-y}\text{Mn}_y\text{O}_x\text{Te}_{1-x}$  alloys that is associated with the lowest  $\Gamma$  conduction band (termed  $E_-$  subband). The pressure-induced energy shift of the  $E_-$  transition is nonlinear and much weaker as compared to the change of the direct band gap of  $\text{Zn}_{0.88}\text{Mn}_{0.12}\text{Te}$ . The weak pressure dependence of the  $E_-$  transition can be fully understood based on the band anticrossing model in which the  $E_-$  subband results from an interaction between the extended  $\text{ZnMnTe}$  conduction-band states and the localized O electronic states. © 2004 American Institute of Physics. [DOI: 10.1063/1.1646457]

The discovery of band anticrossing-induced conduction-band splitting caused by the strong interaction between the extended conduction-band states and localized N resonant states in  $\text{Ga}_{1-x}\text{In}_x\text{N}_y\text{As}_{1-y}$  alloys<sup>1</sup> has led to extensive studies on the properties of so-called highly mismatched alloys (HMAs) in which a small fraction of the constituent anion element is replaced by an element with highly dissimilar properties in terms of electronegativity and atomic size.<sup>2–10</sup> The dramatic changes of the electronic properties caused by substitution of the group V element in group III–V compounds with small amounts of nitrogen at alloylike concentrations, such as a pronounced reduction of the fundamental band-gap energy,<sup>11,12</sup> a significant increase in the electron effective mass and a decrease in the electron mobility,<sup>7,13,14</sup> as well as the appearance of an optical transition ( $E_+$ ) from the valence band to the conduction band at the  $\Gamma$  point,<sup>1,4,15</sup> have been well explained by the band anticrossing (BAC) model.<sup>1,2</sup>

The anticrossing interaction between the extended conduction-band states of a semiconductor matrix and the highly localized electronic states introduced by the isoelectronic substitutional atoms with high electronegativity, such as N in GaAs or O in ZnSe, can be expressed as<sup>1,2</sup>

$$E_{\pm}(k) = \frac{1}{2} \{ (E_M(k) + E_D) \pm \sqrt{(E_M(k) - E_D)^2 + 4V^2} \}, \quad (1)$$

where  $E_M(k)$  and  $E_D$  are the energies of the unperturbed conduction band and of the localized states relative to the top of the valence band, respectively. The matrix element describing the interaction and hybridization between the localized states and the extended conduction-band states  $V = C_{MD}x^{1/2}$ , where  $C_{MD}$  is a constant dependent on the semiconductor matrix and  $x$  is the alloy composition. The energy positions of the subband edges given by Eq. (1) depend on the interaction parameter  $V$  and the location of  $E_D$  with respect to the conduction-band edge  $E_M$ . Illustrated in Fig. 1

are schematic examples of the calculated band structure based on the BAC model. The interaction between the localized isoelectronic states and the extended conduction-band states has a pronounced effect on the dispersion relation of the two conduction subbands  $E_-$  and  $E_+$ . If the localized state is located within the conduction band of the matrix, as depicted in Fig. 1(a), the conduction-band states at the  $E_-$  edge mostly retain the extended  $E_M$ -like character and those at the  $E_+$  edge are more of a localized and  $E_D$ -like character. If the localized states lie below the conduction-band edge, as displayed in Fig. 1(b), the conduction-subband edges  $E_-$  and  $E_+$  switch their characters: The  $E_-$  subband states have the highly localized nature and  $E_+$  subband states possess the character of extended state.

To date, most experimental studies have concentrated on the case of the localized state resonant with the conduction band, such as the well known case of  $\text{GaN}_x\text{As}_{1-x}$ . In this work, we address the case in which the localized state is located below the conduction band and within the forbidden gap of a semiconductor matrix. Specifically, we study the

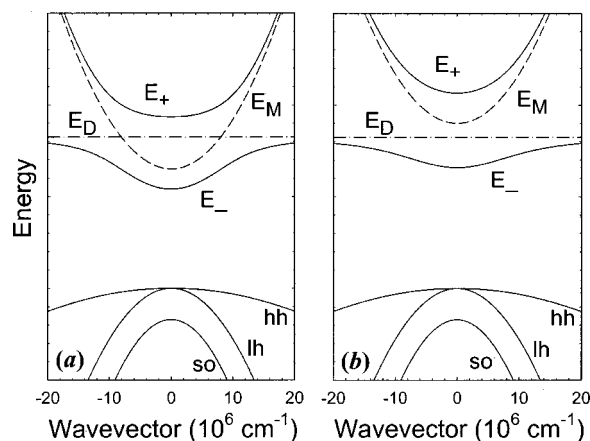


FIG. 1. Illustration of the effects of band anticrossing on the  $\Gamma$  conduction-band structure. (a) The highly electronegative isoelectronic impurity-induced localized state resonant with the conduction band; (b) The localized state located below the conduction band. The solid lines are the restructured  $E_-$  and  $E_+$  subbands resulting from the band anticrossing interaction between the localized states (dashed-dotted line) and the extended states of the conduction band (broken line).

<sup>a)</sup>Electronic mail: wshan@lbl.gov

<sup>b)</sup>Also at: Department of Materials Science and Engineering, University of California, Berkeley, CA 94720.

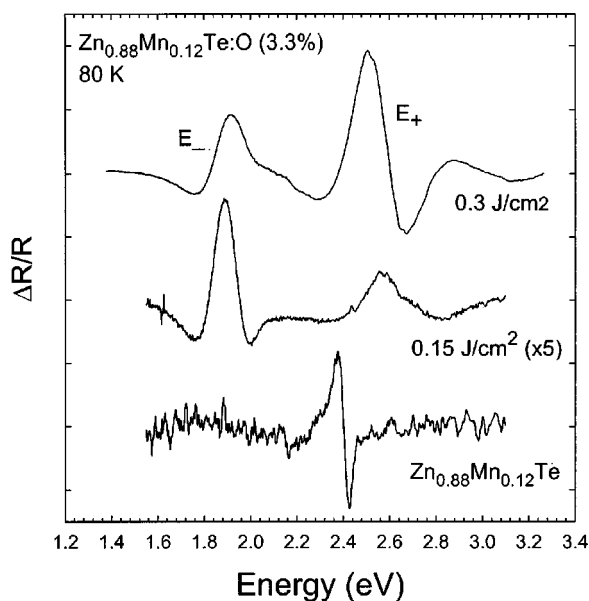


FIG. 2. PR spectra taken from  $\text{Zn}_{0.88}\text{Mn}_{0.12}\text{Te}_{1-x}\text{O}_x$  samples at 80 K compared with the PR curve of  $\text{Zn}_{0.88}\text{Mn}_{0.12}\text{Te}$  substrate.

effect of applied pressure on the band structure of  $\text{Zn}_{1-y}\text{Mn}_y\text{O}_x\text{Te}_{1-x}$  alloys. We show that the formation of  $E_-$  and  $E_+$  bands in  $\text{Zn}_{1-y}\text{Mn}_y\text{O}_x\text{Te}_{1-x}$  can be demonstrated experimentally and the characteristic signature of the  $E_-$  subband edge can be verified unmistakably by its pressure dependence.

The  $\text{Zn}_{1-y}\text{Mn}_y\text{O}_x\text{Te}_{1-x}$  samples used in this work are synthesized using O ion implantation followed by pulsed laser melting (PLM). This approach is very effective in incorporating impurities into a crystal to levels well above the solubility limit due to the rapid recrystallization rate.<sup>16,17</sup> Synthesis of diluted  $\text{Ga}_{1-x}\text{Mn}_x\text{As}_{1-x}$ ,<sup>18</sup> as well as ferromagnetic  $\text{Ga}_{1-x}\text{Mn}_x\text{As}$  (Ref. 19) using the PLM process has recently been demonstrated. Multiple energy implantation using 30 and 90 keV  $\text{O}^+$  ions was carried out into  $\text{Zn}_{0.88}\text{Mn}_{0.12}\text{Te}$  single crystals to form  $\sim 0.2 \mu\text{m}$  thick layers with relatively constant O concentrations corresponding to O mole fractions of 0.0165–0.044. The reason for using ternary  $\text{ZnMnTe}$  as substrates is that the presence of Mn enhances and stabilizes the incorporation of O.<sup>8</sup> The  $\text{O}^+$ -implanted samples were pulsed-laser melted in air using a KrF laser ( $\lambda=248 \text{ nm}$ ) with a pulse duration  $\sim 38 \text{ ns}$ . After passing through a multiprism homogenizer, the fluence at the sample ranged between 0.020 and 0.3  $\text{J}/\text{cm}^2$ .

Photomodulation spectroscopy measurements were carried out to measure the energies of the optical transitions in the samples in both transmission (PT) and reflection [photo-reflectance (PR)] configurations. Quasimonochromatic light from a xenon arc lamp dispersed by a 0.5 m monochromator was focused on the samples as a probe beam. A chopped HeCd laser beam (3250 or 4420 Å) provided the photomodulation. The photomodulated spectral signals were detected by a Si photodiode using a phase-sensitive lock-in amplification system. Application of hydrostatic pressure was accomplished by mounting small sample chips with sizes of  $\sim 200 \times 200 \mu\text{m}^2$  into a gasketed diamond anvil cell.

Figure 2 shows PR spectra taken at 80 K from two  $\text{Zn}_{0.88}\text{Mn}_{0.12}\text{O}_x\text{Te}_{1-x}$  samples implanted with 3.3%  $\text{O}^+$  fol-

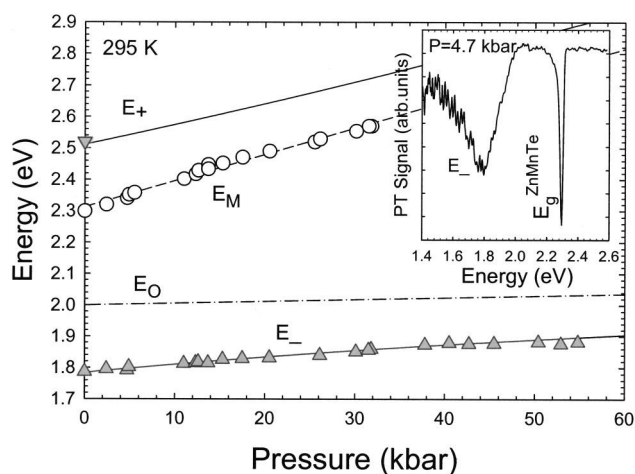


FIG. 3. Effect of pressure on the energy position of the  $E_-$  band edge of a  $\text{Zn}_{0.88}\text{Mn}_{0.12}\text{Te}_{1-x}\text{O}_x$  sample (triangles). The change of the band gap of the  $\text{Zn}_{0.88}\text{Mn}_{0.12}\text{Te}$  substrate with pressure is also displayed (open circle). The solid lines are theoretical fitting results. The dashed-dotted line is the location of  $E_0$  relative to the top of the valence band. The inset shows a typical PT spectrum of  $\text{Zn}_{0.88}\text{Mn}_{0.12}\text{Te}_{1-x}\text{O}_x$  under pressure.

lowed by PLM with laser energy fluences of 0.15 and 0.3  $\text{J}/\text{cm}^2$ , as well as from the  $\text{Zn}_{0.88}\text{Mn}_{0.12}\text{Te}$  used as the substrate in this work. The actual “active” O concentration ( $x$ ) in the  $\text{Zn}_{0.88}\text{Mn}_{0.12}\text{O}_x\text{Te}_{1-x}$  samples is estimated to be roughly around 1%.<sup>20</sup> However, its precise value is not very important in the discussion presented here. The derivative-like spectral feature in the PR spectrum of  $\text{Zn}_{0.88}\text{Mn}_{0.12}\text{Te}$  corresponds to the optical transition from the valence-band edge to the conduction-band edge. The band-gap energy is found to be 2.40 eV at 80 K for the  $\text{Zn}_{0.88}\text{Mn}_{0.12}\text{Te}$  matrix. For the oxygen containing samples, the PR spectra exhibit two features with energies distinctly different from the fundamental band gap of  $\text{Zn}_{0.88}\text{Mn}_{0.12}\text{Te}$  matrix. These two transitions are assigned to those from the top of the valence band to the two conduction subband edges,  $E_-$  ( $\sim 1.85 \text{ eV}$ ) and  $E_+$  ( $\sim 2.6 \text{ eV}$ ), formed by the band anticrossing interaction between the localized O states and the extended conduction-band states of  $\text{ZnMnTe}$  matrix as illustrated by Fig. 1(b). The strong photomodulation signals of both  $E_-$  and  $E_+$  indicate the band-to-band nature of these transitions and suggest that the  $E_-$  transition has substantial oscillator strength comparable to that of the  $E_+$  transition.

To further elucidate the origin of the  $E_-$  band, we have studied the effects of hydrostatic pressure on the  $E_-$  transition. The energy positions of the  $E_-$  transition in the sample treated by PLM with a laser energy fluence of 0.3  $\text{J}/\text{cm}^2$  has been measured as a function of applied hydrostatic pressure at room temperature. The results are shown in Fig. 3, along with the measured pressure dependence of the band gap of the  $\text{Zn}_{0.88}\text{Mn}_{0.12}\text{Te}$  matrix. The room-temperature energy position of the  $E_+$  transition at atmospheric pressure is also shown in Fig. 3. The inset of Fig. 3 shows a typical PT spectrum recorded at high pressures. By fitting the experimental data (open circles in Fig. 3) to  $\Delta E(P) = \alpha P$  with  $\alpha = dE_g/dP$ , the pressure dependence of the  $\text{Zn}_{0.88}\text{Mn}_{0.12}\text{Te}$  band gap is found to be  $dE_g/dP = 8.5 \text{ meV/kbar}$ . It is not surprising to see that the pressure-induced energy shift of the  $E_-$  transition is much weaker (initial slope  $\approx 2 \text{ meV/kbar}$ ) and nonlinear as compared to change of the direct band gap

of  $\text{Zn}_{0.88}\text{Mn}_{0.12}\text{Te}$ . The weak pressure dependence of the  $E_-$  transition can be fully understood with the BAC model. The fact that  $E_-$  is located much closer to the energy level of the localized O states [Fig. 1(b)] gives its wave function a pronounced O-like character. The solid lines through the experimental data in Fig. 3 are the calculated pressure dependencies of  $E_-$  and  $E_+$  transitions using Eq. (1). The best fits to the data yield the energy position of O level (relative to the top of the valence band)  $E_D = E_V + 2.0 \pm 0.1$  eV at atmospheric pressure with a pressure dependence of  $0.6 \pm 0.1$  meV/kbar. It is clear from Fig. 3 that the pressure dependence of the  $E_-$  transition is slightly stronger than that of the O level as expected from the admixture of extended conduction-band  $\Gamma_C$  states of matrix to the  $E_-$  band-edge states. On the other hand, the much weaker pressure dependence of the  $E_-$  transition as compared to that of the conduction-band  $\Gamma_C$  edge indicated the predominantly O-like nature of the  $E_-$  band.

The present results have important inferences for the understanding of the origin of the unusual electronic structure of HMAs. They show that the electronic structure of different HMAs can be explained by the BAC model with a common picture. They also provide strong arguments against other previously proposed models. It has been argued that the electronic structure of  $\text{GaN}_x\text{As}_{1-x}$  alloys results from an interaction between the closely lying  $\Gamma_C$ ,  $L_C$ , and  $X_C$  minima.<sup>21–23</sup> The interaction is caused by the perturbation potential resultant from the substitution of a N atom to an As atom. In these models, the smaller and pressure dependent pressure coefficient of the  $E_-$  transition observed in  $\text{GaN}_x\text{As}_{1-x}$  alloys was attributed to the increasing contribution of the  $L_C$  and  $X_C$  minima whose pressure coefficients are much smaller than that of the  $\Gamma_C$  minimum. Apparently, these models cannot explain the results presented here. The large downward shift of 0.5 eV of the conduction-band minimum ( $E_-$ ) and the very weak pressure dependence of the band energy as shown in Fig. 3 cannot be attributed to the influence from the conduction-band  $L$  and  $X$  edges because they are located far away from the  $\Gamma_C$  edge ( $>1.0$  eV) in  $\text{Zn}_{1-y}\text{Mn}_y\text{Te}$ .<sup>24</sup> Thus, our results directly confirm that the  $E_-$  transition together with the  $E_+$  are the results of a band anticrossing interaction between the extended  $\Gamma$  conduction-band states and highly localized states in highly mismatched alloys.

In conclusion, we have studied the effect of pressure on the electronic band structure of  $\text{Zn}_{1-y}\text{Mn}_y\text{O}_x\text{Te}_{1-x}$  alloys by investigating the optical transitions associated with the  $\Gamma$  point at the conduction-band and the valence-band edges. The  $\text{Zn}_{1-y}\text{Mn}_y\text{O}_x\text{Te}_{1-x}$  samples were found to exhibit a classical band-anticrossing behavior with the formation of two conduction subbands ( $E_-$  and  $E_+$ ) resulting from the strong interaction between the extended conduction-band states of  $\text{Zn}_{1-y}\text{Mn}_y\text{Te}$  and the localized O states. By exam-

ining the effect of applied pressure on the  $E_-$  transition, we are able to derive the energetic position of  $E_D = E_V + 2.0 \pm 0.1$  eV for the localized O level and its pressure dependence of  $0.6 \pm 0.1$  meV/kbar from the experimental results.

This work is supported by the Director, Office of Science, Office of Basic Energy Sciences, Division of Materials Sciences and Engineering, of the U.S. Department of Energy under Contract No. DE-AC03-76SF00098.

- <sup>1</sup>W. Shan, W. Walukiewicz, J. W. Ager III, E. E. Haller, J. F. Geisz, D. J. Friedman, J. M. Olson, and S. R. Kurtz, Phys. Rev. Lett. **82**, 1221 (1999).
- <sup>2</sup>W. Walukiewicz, W. Shan, J. W. Ager III, D. R. Chamberlin, E. E. Haller, J. F. Geisz, D. J. Friedman, J. M. Olson, and S. R. Kurtz, in *Photovoltaics for the 21st Century*, edited by V. K. Kapur, R. D. McDonnell, D. Carlson, G. P. Ceasar, and A. Rohatgi (Electrochemical Society, Pennington, NJ, 1999), p. 199.
- <sup>3</sup>A. Lindsay and E. P. O'Reilly, Solid State Commun. **112**, 443 (1999).
- <sup>4</sup>W. Shan, W. Walukiewicz, J. W. Ager, E. E. Haller, J. F. Geisz, D. J. Friedman, J. M. Olson, and S. R. Kurtz, J. Appl. Phys. **86**, 2349 (1999).
- <sup>5</sup>P. J. Klar, H. Grüning, W. Heimbrodt, J. Koch, F. Höhnsdorf, W. Stolz, P. M. A. Vicente, and J. Camassel, Appl. Phys. Lett. **76**, 3439 (2000).
- <sup>6</sup>W. Walukiewicz, W. Shan, K. M. Yu, J. W. Ager III, E. E. Haller, I. Miotkowski, M. J. Seong, H. Alawadhi, and A. K. Ramdas, Phys. Rev. Lett. **85**, 1552 (2000).
- <sup>7</sup>C. Skierbiszewski, P. Perlin, P. Wisniewski, W. Knap, T. Suski, W. Walukiewicz, W. Shan, K. M. Yu, J. W. Ager, E. E. Haller, J. F. Geisz, and J. M. Olson, Appl. Phys. Lett. **76**, 2409 (2000).
- <sup>8</sup>K. M. Yu, W. Walukiewicz, J. Wu, J. W. Beeman, J. W. Ager III, E. E. Haller, I. Miotkowski, A. K. Ramdas, and P. Becla, Appl. Phys. Lett. **80**, 1571 (2002).
- <sup>9</sup>J. Wu, W. Shan, and W. Walukiewicz, Semicond. Sci. Technol. **17**, 860 (2002).
- <sup>10</sup>W. Shan, W. Walukiewicz, J. W. Ager III, K. M. Yu, J. Wu, E. E. Haller, Y. Nabetani, T. Mukawa, Y. Ito, and T. Matsumoto, Appl. Phys. Lett. **83**, 299 (2003).
- <sup>11</sup>M. Weyers, M. Sato, and H. Ando, Jpn. J. Appl. Phys., Part 2 **31**, L853 (1992).
- <sup>12</sup>M. Kondow, K. Uomi, K. Hosomi, and T. Mozume, Jpn. J. Appl. Phys., Part 2 **33**, L1056 (1994).
- <sup>13</sup>J. F. Geisz, D. J. Friedman, J. M. Olson, S. R. Kurtz, and M. B. Keyes, J. Cryst. Growth **195**, 401 (1998).
- <sup>14</sup>S. R. Kurtz, Allerman, C. H. Seager, R. M. Sieg, and E. D. Jones, Appl. Phys. Lett. **77**, 400 (2000).
- <sup>15</sup>J. D. Perkins, A. Mascaranhas, Y. Zhang, J. F. Geisz, D. J. Friedman, J. M. Olson, and S. R. Kurtz, Phys. Rev. Lett. **82**, 3312 (1999).
- <sup>16</sup>C. W. White and P. S. Peercy, eds., *Laser and Electron Beam Processing of Materials* (Academic, New York, 1980).
- <sup>17</sup>J. S. Williams, in *Laser Annealing of Semiconductors*, edited by J. M. Poate and J. W. Mayer (Academic, New York, 1982), p. 385.
- <sup>18</sup>K. M. Yu, W. Walukiewicz, M. A. Scarpulla, O. D. Dubon, J. Jasinski, Z. Liliental-Weber, J. Wu, J. W. Beeman, M. R. Pillai, and M. J. Aziz, J. Appl. Phys. **94**, 1043 (2003).
- <sup>19</sup>M. A. Scarpulla, K. M. Yu, O. Monteiro, M. Pillai, M. C. Ridgway, M. J. Aziz, and O. D. Dubon, Appl. Phys. Lett. **82**, 1251 (2003).
- <sup>20</sup>K. M. Yu, W. Walukiewicz, J. Wu, W. Shan, J. W. Beeman, M. A. Scarpulla, O. D. Dubon, and P. Becla (unpublished).
- <sup>21</sup>E. D. Jones, N. A. Modine, A. A. Allerman, S. R. Kurtz, A. F. Wright, S. T. Tozer, and X. Wei, Phys. Rev. B **60**, 4430 (1999).
- <sup>22</sup>T. Mattila, S. H. Wei, and A. Zunger, Phys. Rev. B **60**, R11245 (1999).
- <sup>23</sup>N. G. Szvacki and P. Boguslawski, Phys. Rev. B **64**, 16201 (2001).
- <sup>24</sup>*Landolt-Börnstein*, edited by O. Madelung and M. Schultz, New Series, Group 3, Vol. 22, Part a (Springer, Berlin, 1988).